Fuel 132 (2014) 194–203

Contents lists available at ScienceDirect

Fuel

journal homepage: www.elsevier.com/locate/fuel

Benchmark assessment of coal permeability models on the accuracy of permeability prediction

Yan Peng [a,b], Jishan Liu [b,*], Wancheng Zhu [c], Zhejun Pan [d], Luke Connell [d]

[a] State Key Laboratory of Geomechanics and Geotechnical Engineering, Institute of Rock and Soil Mechanics, Chinese Academy of Sciences, Wuhan 430071, China
[b] School of Mechanical and Chemical Engineering, The University of Western Australia, 35 Stirling Highway, Crawley, WA 6009, Australia
[c] Key Laboratory of Ministry of Education on Safe Mining of Deep Metal Mines, Northeastern University, Shenyang 110819, China
[d] CSIRO Earth Science and Resource Engineering, Private Bag 10, Clayton South, Victoria 3169, Australia

HIGHLIGHTS

- Performances of coal permeability models were benchmarked against correct solutions.
- Assumptions of uniaxial stress, constant overburden stress and local equilibrium were removed.
- The effective stress transfer between matrix and fracture were included.
- These three assumptions were identified as the reason of coal permeability model failures.

ARTICLE INFO

Article history:
Received 10 January 2014
Received in revised form 18 March 2014
Accepted 23 April 2014
Available online 9 May 2014

Keywords:
Benchmark assessment
Coal permeability
Boundary effects
Local equilibrium

ABSTRACT

When natural gas is extracted from coal seams, complex interactions of stress and sorptive chemistry have a strong influence on the properties of coal. These include influences on gas sorption and flow, coal deformation, porosity change and permeability modification. In this study, we define this chain of reactions as "coupled processes" implying that one physical process affects the initiation and progress of another. The individual process, in the absence of full consideration of cross couplings, forms the basis of the conventional coal seam gas reservoir engineering. Therefore, the inclusion of cross couplings is the key to rigorously formulate the unconventional coal seam gas reservoir engineering. Among those cross-couplings, the coal permeability model is the most important one. A variety of permeability models were developed to define how the coal permeability evolves during gas production. These models were derived normally under three common assumptions: (1) uniaxial strain; (2) constant overburden stress; and (3) local equilibrium. Under these assumptions, coal permeability can be defined as a function of gas pressure only. Our comprehensive review concluded that these models have so far failed to explain experimental results from conditions of the controlled stresses, and only partially succeeded in explaining in situ data. We identified the adoption of these three assumptions as the fundamental reason for failures. In this study, we relaxed the first two assumptions and derived a coal permeability model under variable stress conditions. Furthermore, we considered the effective stress transfer between matrix and fracture and transformed this stress transfer into the modification of fracture aperture. This relaxes the third common assumption, i.e., local equilibrium condition. We applied this approach to generate a series of permeability type curves under the full spectrum of boundary conditions spanning prescribed stresses through constrained displacement. We benchmarked the solutions generated by using the permeability models with three common assumptions against our "accurate" solutions by using permeability models without these assumptions for the full spectrum of boundary conditions, and concluded that these common assumptions could produce unacceptable errors.

1. Introduction

From in situ and experimental observations, permeability of a coal seam gas reservoir is not constant during depletion of the coal-bed methane (CBM) since gas extractions trigger complicated

* Corresponding author. Tel.: +61 8 6488 7205; fax: +61 8 6488 1964.
E-mail address: jishan.liu@uwa.edu.au (J. Liu).

http://dx.doi.org/10.1016/j.fuel.2014.04.078

gas–coal interactions. Acid gases like methane originally adsorb around surface of coal, causing a sorption-induced strain in reservoirs. When CBM is extracted from coal seams, gas desorbs from coal surface and coal matrix shrinks. This coal matrix shrinkage may increase coal permeability while the rising effective stress due to the drop of pore pressure can lead to the decline of permeability [1,2]. Furthermore, other factors, like heterogeneity of coal, gas composition and water content, also contribute to the complexity of gas–coal interactions [3–5]. All of these lead to permeability hardly be predicted and change dramatically: up to 100 times in the San Juan basin [6]. Moreover, permeability of a reservoir has a close relationship with productivity of CBM. Information on permeability is in favor of long-term production design. However to obtain information on permeability in the field is very expensive since it requires multi-well tests [7]. Therefore, a mathematical model of determining changes in permeability is very valuable.

A number of permeability models for coal have been proposed under specific assumptions. Table 1 lists current permeability models and their assumptions. Uniaxial strain and constant overburden stress are regarded as usual boundary conditions in reservoirs. Most of early permeability models were proposed based on these two assumptions. Gray [8] first incorporated the effect of matrix shrinkage into permeability model and considered effective horizontal stresses controlled changes of permeability. Gilman and Beckie [9] presented a simplified geometry model for CBM and corresponding mathematical model of permeability which also contains the release mechanism of methane from matrix into cleats. Shi and Durucan [10] improved the model proposed by Gray and considered the volumetric matrix shrinkage is proportional to the volume of desorbed gas rather than to reduction in the equivalent sorption pressure. Palmer and Mansoori [11] (called as P&M model later) derived a widely used theoretical permeability model which is a function of effective stress and matrix shrinkage. The P&M model was improved and summarized by Palmer et al. [12]. The geometry of all these models except Gilman and Beckie model that had a simplified geometry was matchsticks model.

Usually, the uniaxial strain condition is invalid in laboratory. To obtain permeability suitable for laboratory conditions, cubic geometry model instead of matchsticks geometry was applied. Schwerer and Pavone [13] developed a permeability model for laboratory measurements under the constant overburden stress condition. Pekot and Keeves [14] improved that model, considering the effect of matrix shrinkage on the permeability. They assumed that matrix shrinkage was proportional to the adsorbed gas concentration change multiplied by shrinkage compressibility. Roberson and Christiansen [15] further relaxed the constant overburden stress assumption and presented a new equation that can be used to model the permeability behavior of a fractured, sorptive-elastic media under variable stress conditions commonly used during measurement of permeability data in the laboratory. From constitutive relation for poroelastic media, Cui and Bustin [16] developed a general stress-based porosity and permeability model for deep coal seams, considering effects of reservoir pressure and sorption-induced volumetric strain on permeability.

Currently, it was pointed out that constant overburden stress condition is invalid near the wellbore. The stress arching exists above a wellbore due to the cylindrical hole not supporting any overburden directly above it [17]. Therefore, permeability models under usual assumptions may be inaccurate for reservoirs. In recent years, significant efforts have been made to develop permeability models without those usual assumptions. Gu and Chalaturnyk [18] proposed a permeability model. It overcame the usual assumptions and could reflect anisotropy in permeability and deformation. Following the similar method with Cui and Bustin, Zhang et al. [19] developed a strain-based porosity and permeability model based on theory of poroelasticity. It was shown that current commonly used permeability models could be treated as specific examples. Connell et al. [20] proposed two new analytical permeability models representing for standard triaxial strain and stress conditions.

Siriwardane et al. [21] conducted experiments and showed that permeability of adsorbing gas in coal is a function of exposure time. According to this, Liu et al. [22] believed that permeability changes related to the process of gas–coal interactions and proposed a permeability switching model. They explained why permeability under the influence of gas adsorption can switch instantaneously from reduction to enhancement and revealed the transition of coal matrix swelling from local swelling to macro-swelling under the unconstrained swelling condition. In accordance with their theory, all the other above permeability models have the other assumption: local equilibrium, which means that those models ignored dynamic interactions between matrix deformation and fracture aperture alternation. Currently, the conceptual dual porosity model was proposed by Wu et al. [23,24] and it could involve the effect of interactions between two systems on fracture permeability. Nevertheless, the permeability model used in this method was also the common one with the above assumption of local equilibrium.

As reviewed above, a wide variety of coal permeability models have been proposed. However, these models have only partially succeeded in explaining in situ data. Even like P&M model which is used widely to match in situ data among permeability models, its improved formation could match two different sets of San Juan data only with three rigorous preconditions [6]. Compared with experimental data, these models have so far failed to explain experimental results from conditions of the controlled stresses and even could not match the trend of experimental data. To solve this issue, Robertson and Christiansen [25] added a strain factor into these models. Results from these improved models had consistent trends with experimental observations but the

Table 1
Summary of current permeability models and their assumptions.

Proposed by	Assumption		
	Uniaxial strain	Constant overburden stress	Local equilibrium
Gray [8]	√	√	√
Gilman and Beckie [9]	√	√	√
Shi and Durucan [10]	√	√	√
Palmer et al. [11,12]	√	√	√
Schwerer and Pavone [13]		√	√
Pekot and Keeves [14]		√	√
Roberson and Christiansen [15]			√
Cui and Bustin [16]			√
Gu and Chalaturyk [18]			√
Zhang et al. [19]			√
Connell et al. [20]			√

deviation between experimental data and prediction calculated by these models could not be ignored and sometimes it came out to be 60%. Liu et al. [2,26] regarded this mismatch between current theoretical models and experimental data is due to the ignorance of the internal actions between coal fractures and matrix. Moreover, dynamic interactions process has a significant impact on the permeability change. Their further research [22] considering dynamic interactions obtained the reasonable result which was consistent with typical laboratory and in situ observations available in literatures.

From above analysis, we believe that three common assumptions are the fundamental reason for failures of current permeability models to correctly explain the experimental observations. In this study, we used our poroelastic permeability model to relax the first two assumptions (uniaxial strain and constant overburden stress) and built explicit 3-D simulations to relax the third assumption (local equilibrium). These simulations contained the dynamic interactions between coal matrix swelling/shrinkage and fracture aperture alteration and translations of these interactions to permeability evolution under full spectrum of boundary conditions. Through these, we benchmarked the solutions generated by the P&M permeability model with three common assumptions against our *accurate* solutions by the permeability model without these assumptions for the full spectrum of boundary conditions, and concluded that these three common assumptions could produce unacceptable errors.

2. Methodology

To relax two usual assumptions: uniaxial strain and constant overburden stress, the general strain-based porosity and permeability models derived by Zhang et al. [19] are applied to the following numerical simulations under variable boundary conditions and its solutions are regarded as *accurate solutions* in this study. In this model, the coal porosity ratio evolves with the effective strain increment as:

$$\frac{\phi}{\phi_0} = 1 + \frac{\alpha}{\phi_0}\Delta\varepsilon_e \tag{1}$$

There is a relationship between porosity, permeability and the grain-size distribution in porous media. Chilingar [27] defined this relationship as:

$$k = \frac{d_e^2\phi^3}{72(1-\phi)^2} \tag{2a}$$

where k is the permeability, ϕ is the porosity and d_e is the effective diameter of grains.

Based on this equation, one obtains

$$\frac{k}{k_0} = \left(\frac{\phi}{\phi_0}\right)^3\left(\frac{1-\phi_0}{1-\phi}\right)^2 \tag{2b}$$

The cubic relationship between permeability and porosity for the coal matrix is valid when the porosity is much smaller than 0.1 (normally less than 10%):

$$\frac{k}{k_0} = \left(\frac{\phi}{\phi_0}\right)^3 \tag{2c}$$

Substituting Eq. (1) into (2c), the permeability ratio is:

$$\frac{k}{k_0} = \left(1 + \frac{\alpha}{\phi_0}\Delta\varepsilon_e\right)^3 \tag{3}$$

where the effective strain increment is calculated by:

$$\Delta\varepsilon_e = \Delta\varepsilon_v + \frac{\Delta p}{K_s} - \Delta\varepsilon_s \tag{4}$$

where $\Delta\varepsilon_e$ is defined as the total effective volumetric strain increment, $\Delta\varepsilon_v$ is total volumetric strain increment, $\Delta p/K_s$ is coal compressive strain change, $\Delta\varepsilon_s$ is gas sorption-induced volumetric strain increment and K_s represents the bulk modulus of coal grains.

Various studies have identified the most important factors influencing adsorption capacity of coal include coal type, rank, moisture content, temperature and pressure [28–33]. This adsorption could induce swelling of coal matrix. Levine [28] used a Langmuir form of equation to describe the swelling and achieved good agreement with the experimental measurements. Although the magnitude of swelling due to adsorption was different for different coal types and ranks, the swelling isotherms showed similar trends [29–32]. Moreover, Clarkson and Bustin [33] suggested that the Dubinin–Astakhov equation provides a better fit to coal gas isotherm data, particularly for carbon dioxide, than the conventionally used Langmuir equation at high pressure. However the Dubinin–Astakhov equation also has a same trend with Langmuir equation.

No matter what the equation describing the adsorption isotherms is used, the trend of gas transport will be same and the effect of coal swelling due to adsorption on permeability will be same. In this study, the Langmuir model, a relatively simple model, is used to describe the low-pressure adsorption behavior:

$$\varepsilon_s = \varepsilon_L\frac{p}{P_L + p} \tag{5}$$

where ε_L is a constant representing the volumetric strain at infinite pore pressure and the Langmuir pressure constant, P_L representing the pore pressure at which the measured volumetric strain is equal to 0.5 ε_L.

Based on linear elastic mechanics, the total volumetric strain can be obtained by the deformation component and it is defined as:

$$\varepsilon_v = \varepsilon_{11} + \varepsilon_{22} + \varepsilon_{33} + \varepsilon_{11}\varepsilon_{22} + \varepsilon_{11}\varepsilon_{33} + \varepsilon_{22}\varepsilon_{33} + \varepsilon_{11}\varepsilon_{22}\varepsilon_{33} \tag{6a}$$

This study deals with elastic small strain problem and three principal strains are relatively tiny. The products of principal strains are much smaller than principal strains themselves so they could be ignored. The volumetric strain could be simplified as:

$$\varepsilon_v = \varepsilon_{11} + \varepsilon_{22} + \varepsilon_{33} \tag{6b}$$

where ε_{11}, ε_{22} and ε_{33} are three principal strains obtained from numerical simulations.

As a counterpart, permeability models with usual assumptions are regarded as "industry-standard" permeability models in this study. Among them, the P&M model derived by Palmer–Mansoori [11] is popular one so the following simulations use it as the representative of "industry-standard" models. The P&M model is defined as:

$$\frac{k}{k_0} = \left[1 + \frac{1}{M\varphi_0}(p - p_0) + \frac{\varepsilon_L}{\varphi_0}\left(\frac{K}{M} - 1\right)\left(\frac{p}{P_L + p} - \frac{p_0}{P_L + p_0}\right)\right]^3 \tag{7}$$

where $M = \frac{E(1-\nu)}{(1+\nu)(1-2\nu)}$ and E is Young's modulus of coal and ν is Possion's ratio of coal.

It also can be expressed as:

$$\frac{k}{k_0} = \left[1 + \frac{1}{\varphi_0}(\Delta\varepsilon_{33} - \Delta\varepsilon_s)\right]^3 \tag{8}$$

3. Representation of coal matrix–fracture interactions

Coal is a typical dual porosity/permeability system containing porous matrix surrounded by fracture. In this study, we consider the interactions between fracture and matrix system and use a conceptual geometry model proposed by Liu et al. [2]. In this model, coal matrix blocks are connected to each other by coal-matrix bridges. The evolution of the fracture permeability change is related to change of fracture aperture. The definition of fracture permeability is as:

$$\frac{k_f}{k_{f0}} = \left(1 + \frac{\Delta b}{b_0}\right)^3 \tag{9}$$

where b_0 is initial fracture aperture and Δb is change of fracture aperture.

In this model, the matrix swelling strain can generate the internal stress which plays a significant role in the fracture aperture [2,34]. Moreover, this matrix swelling has two stages: local swelling and macro swelling [22]. Initially a coal is in the initial equilibrium state. When gas is injected, the fracture pressure reaches the injection pressure much faster than the matrix pressure and as a consequence the maximum imbalance between matrix pressure and fracture pressure is achieved. This imbalance diminishes as the gas penetrates into the coal matrix which makes the pore pressure increase. At this stage, the coal matrix swells but this swelling is confined in the vicinity of the fracture voids. This localized swelling reduces the fracture aperture thus the fracture permeability drops immediately. As the gas penetration progresses, the swelling zone extends further into the coal matrix. When the swelling zone front moves away from the fracture void, the impact of matrix swelling on the fracture aperture starts to decline. At this stage, the local swelling becomes the macro-swelling and the fracture permeability recovers. When matrix pressure equals fracture pressure again, the final equilibrium state is achieved.

As reviewed in introduction, current permeability models assume that the local equilibrium condition is reached instantly, i.e., the matrix pressure is equalized to the fracture pressure. Under this assumption, the dynamic evolution of fracture permeability could not be captured. To relax this assumption, the special internal boundary called thin elastic layer presenting the coal-matrix bridges between matrix and fracture system is applied into following numerical simulations and it can simulate dynamic interactions between matrix and fractures. The boundary of the thin elastic layer connects two faces like spring shown as Fig. 1. The faces named as a and b are upper and bottom edge of fracture, respectively. The displacement of those two faces means the displacement of two edges of a fracture. Therefore, the change of the fracture aperture can be calculated. Most significantly the thin elastic layer also provides the internal stress proposed by Liu and Rutqvist [34], simulating real internal interactions caused by coal-matrix bridges. In order to make two forces produced by the bridge and the thin elastic layer respectively equal, the spring constant k can be set by the following method.

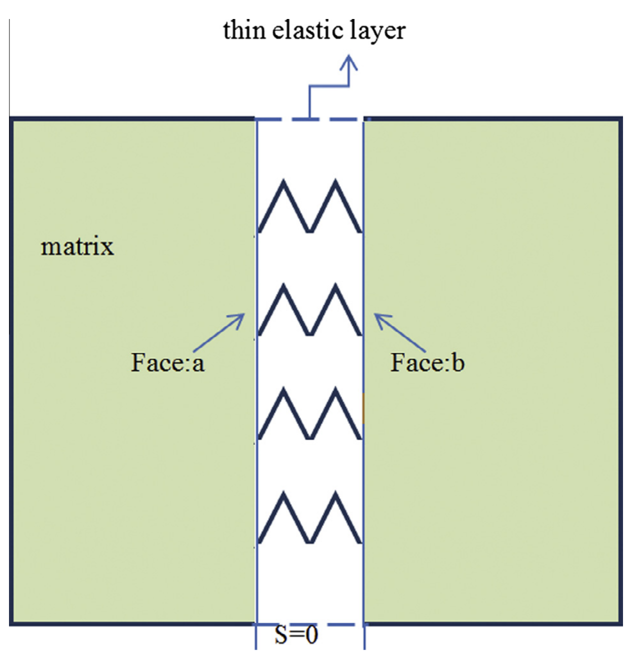

Fig. 1. Illustration of thin elastic layer.

The volumetric strain–stress relationship of coal-matrix bridges is defined as:

$$\Delta\varepsilon_{vb}K = 3\frac{\Delta l_b}{l_{b0}}K = \sigma_b = \frac{3F_b}{A_b} \tag{10}$$

where $\Delta\varepsilon_{vb}$ is volumetric strain of coal-matrix bridges, Δl_b is the strain of coal-matrix bridges, F_b is the internal force provides by coal-matrix bridges, A_b is the area of coal-matrix bridges, σ_b is total internal stress of coal-matrix bridges and l_{b0} is the initial height of coal-matrix bridges.

Simplified Eq. (10) and it can be written as:

$$\frac{\Delta l_b}{l_{b0}}K = \frac{F_b}{A_b} \tag{11}$$

The force produced by the thin elastic layer is defined as:

$$F_e = \int_\Omega ku d\Omega = kuA_e \tag{12}$$

where u is the displacement difference between two connecting faces, A_e is the area of fracture and k is spring constant per unit area.

In fact $u = \Delta l_b$ and $F_b = F_e$. Substituting these two equations and Eq. (12) into Eq. (11), k can be derived as:

$$k = \frac{K}{l_{b0}} \times \frac{A_b}{A_e} \tag{13}$$

Usually the area of bridge occupies only litter in the fracture. In this study we consider that $A_b/A_e = 1/100$.

4. Benchmark assessments of coal permeability models

In order to relax all three common assumptions (uniaxial strain, constant overburden stress and local equilibrium), we built a 3D model to simulate the evolution of coal permeability. In all these simulations, we applied the strain-based permeability model [19] to the simulations. Because this permeability model is valid for variable stress conditions, we consider the permeability solutions as *accurate solutions* while solutions obtained from the P&M model are regarded as *approximate solutions* for permeability models with these three common assumptions. In the following, we present simulation results to quantitatively analyze errors caused by the assumptions.

The model geometry shown as Fig. 2 is a cylinder that the height is 0.1 m and the radius is 0.025 m and the fracture locates at the center. No flow boundary is applied on all the faces and a time-dependent injection pressure, $P_{in}(t)$, is specified at the boundary of fracture. The initial pressure in the matrix is P_0. The special internal boundary condition called thin elastic layer is applied on the fracture. Fig. 2(a) represents the constant volume condition in which all the external boundaries are constrained. Fig. 2(b) shows the uniaxial strain condition in the z-direction. Fig. 2(c) represents the free swelling condition and Fig. 2(d) shows the uniaxial strain condition in the y-direction.

Input parameters for simulations are listed in Table 2. For the gas transport model, $P_{in}(t)$ is defined as:

$$P_{in} = \begin{cases} P_0 + P_d\left(1 - e^{-\frac{t-t_p}{t_d}}\right) & t \geqslant t_p \\ P_0 & t < t_p \end{cases}$$

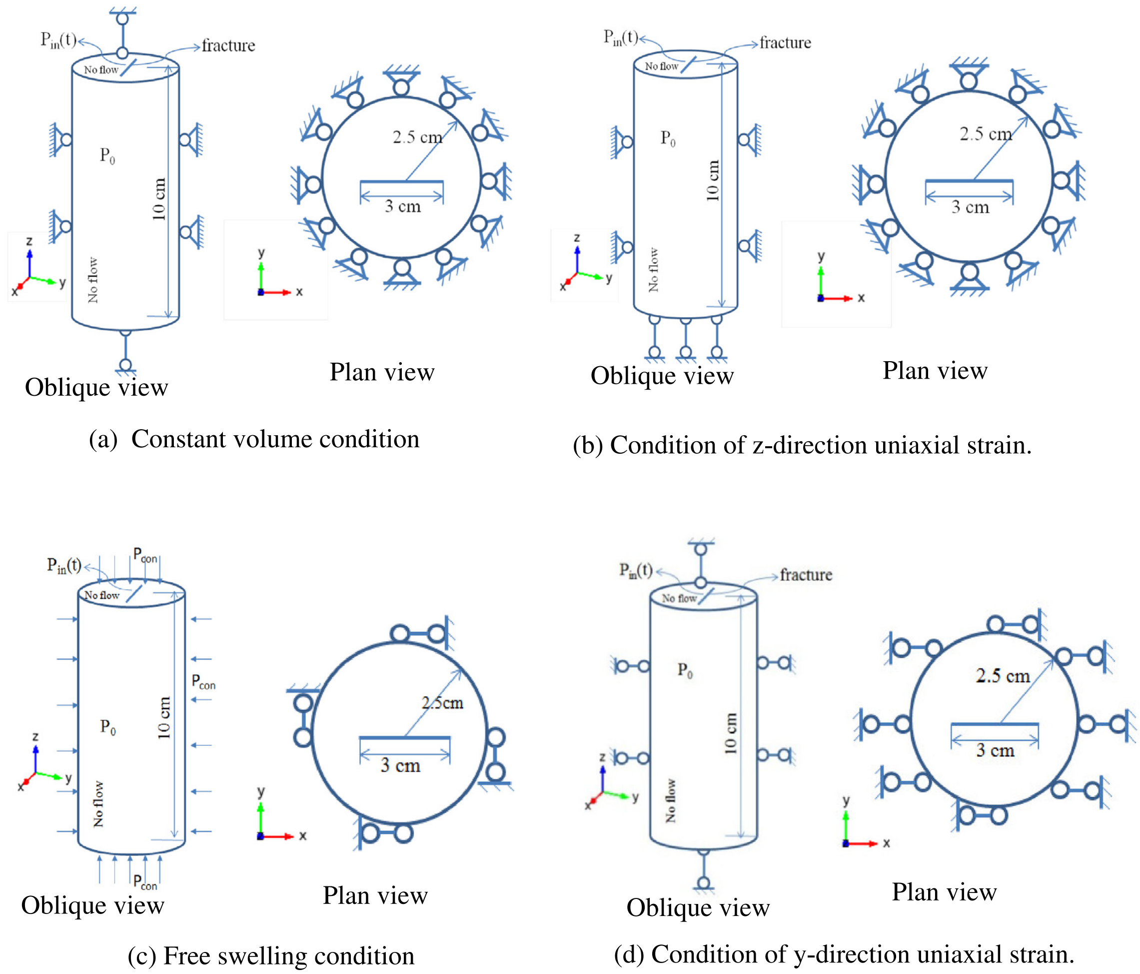

Fig. 2. Simulation models.

Table 2
Input parameters for simulations.

Parameter	Value
Matrix porosity (%)	5.0
Matrix permeability (m^{-2})	10^{-20}
Gas viscosity (Pa s)	1.2278×10^{-5}
Young's modulus (GPa)	6
Possion ratio	0.1
Biot's coefficient	1
Coal density (kg/m^{-3})	1500
Langmuir swelling strain	0.02
Langmuir sorption constant (m^3/kg)	0.01316
Langmuir pressure P_L (MPa)	3.96
Initial pressure (MPa)	0.1
Spring constant in fracture (N/m^3)	164
Pressure increment P_d (MPa)	10
Characteristic time t_d (s)	1250
Start time t_p (s)	5
Initial fracture aperture b_0 (mm)	0.2

where P_d is the pressure increment due to injection. The time t_d is the characteristic time to control loading speed. When the time is less than t_p, no additional loading is applied.

During the production or injection process, the dynamic interactions between matrix and fractures occur due to the existing differential pressure between matrix and fracture. After the differential pressure vanishes, the coal returns its equilibrium state. This dynamic interaction between matrix and fractures plays the key role in coal permeability evolutions. However, assumptions of current permeability models strongly influence this dynamic interaction. The following numerical simulations investigate how the dynamic interaction between matrix and fractures impacts the evolutions of matrix and fracture permeability. Two different permeability models—P&M model and Zhang model—are used to represent the matrix permeability. As shown in Equ.9, the fracture permeability is calculated from its aperture. In this way, the impact of usual assumptions on the matrix and fracture permeability can be quantified.

4.1. Evaluation of boundary condition impacts

4.1.1. Impact on the matrix permeability

The P&M model only considers one scenario: coal matrix is under the condition of uniaxial strain and constant stress in the same direction. In this case, matrix permeability (Eq. (7)) obtained from the P&M model only relates to the pore pressure. Among four scenarios in this study, only the scenario of uniaxial strain under the *y*-direction matches the boundary condition requirements of the P&M model.

Zhang model is the general form without any imposed boundary conditions so theoretically it can be applied to all scenarios. If Zhang model is applied to the same boundary conditions as the P&M model, it would degrade to that model. Fig. 3 shows comparison results of Zhang model with P&M model for this special situation. It is apparent that matrix permeability ratios of Zhang model and P&M model are exactly identical. It indicates that Zhang model successfully transforms to P&M model.

In other cases, boundary conditions differ from the requirements of P&M model. P&M model is no longer valid and could bring errors in matrix permeability ratios while Zhang model gives correct solutions. Fig. 4 illustrates different profiles of the matrix permeability ratio calculated by Zhang model under different boundary conditions. There are significant deviations in matrix permeability ratios between different boundary conditions. As above analysis, P&M model only relates to the pore pressure and as a result, it would get constant matrix permeability ratios for the same pore pressure under different boundary conditions. Consequently, using P&M model would cause unacceptable errors in matrix permeability. Table 3 lists results of steady matrix permeability ratios obtained from these two models under different boundary conditions. For the free swelling condition, P&M model nearly causes 100% deviation in the matrix permeability ratio. Moreover, it also causes 11% and 31% deviations for the *z*-direction uniaxial strain and the constant volume cases, respectively.

4.1.2. Impact on fracture permeability

The impact on the matrix permeability can be transformed directly to the evolution of fracture permeability. Fracture permeability ratios are measured by alternations in fracture apertures as shown in Eq. (9). Moreover, fracture apertures depend on the mechanical behavior of matrix and matrix–fracture bridges and this mechanical behavior is dramatically affected by boundary conditions. Consequently, different boundary conditions may have completely different profiles of fracture permeability ratios.

Fig. 5 compares the results of Zhang model with those of P&M model under the condition of free swelling. Although two solutions have same trends for fracture permeability ratios, they have enormous deviations in magnitudes. The minimum fracture permeability ratio from P&M model is 81% while that value from Zhang model is sharply down to 46%. The huge deviation between them accounts for 76% of the minimum fracture permeability ratio from Zhang model. However, there is only a slight difference between their steady fracture permeability ratios and this small deviation is less than 1%.

Results of fracture permeability ratios from Zhang model and P&M model under the constant volume case are shown in Fig. 6. In this case, two solutions have a moderate deviation. The highest deviation in fracture permeability ratio is only 6.5% and the deviation in minimum fracture permeability ratio is less than 1%. Although this deviation value is small, the error caused by

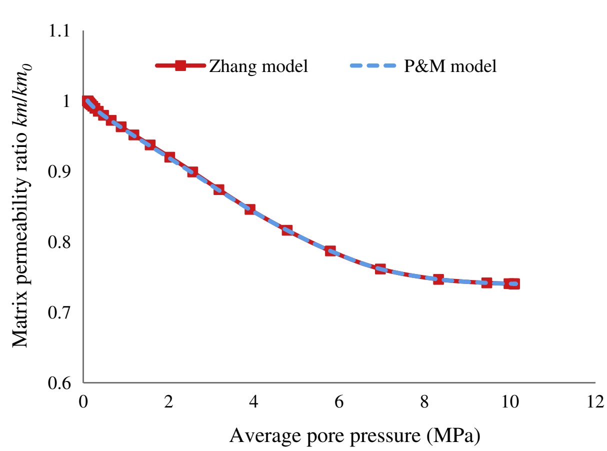

Fig. 3. Evolutions of matrix permeability under the *y*-direction uniaxial strain scenario.

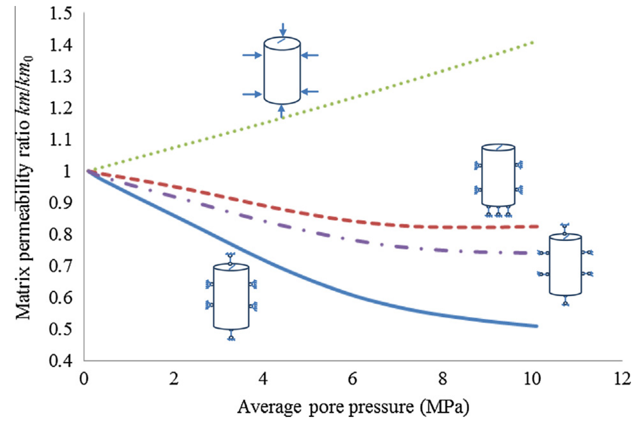

Fig. 4. Summary of matrix permeability ratios for Zhang model under different boundary conditions.

Table 3
Summary of difference in stable matrix permeability ratio (%) for different models.

Models	Boundary Condition			
	Constant volume	*Z*-direction uniaxial strain	Free swelling	*Y*-direction uniaxial strain
P&M model	74	74	74	74
Zhang model	51	82	141	74

assumptions of P&M model is extremely large. Their deviation in minimum fracture permeability ratio is two times larger than the minimum value from Zhang model. Additionally, the same happens to results under the *z*-direction uniaxial strain scenario as shown in Fig. 7. Compared with the Zhang model, P&M model has a higher value in minimum fracture permeability ratio (5.5%) which is 5% higher than that of the Zhang model (0.3%). The largest deviation between these two solutions is 23% when the pore pressure is 2.6 MPa.

From all these four simulations, it is found that evolutions of the matrix permeability ratio of P&M model for various conditions are same. Obviously it is incorrect and having assumptions of uniaxial strain and constant overburden stress results in these obvious faults for P&M model. However, Zhang model considers all effects of boundary condition so evolutions of the matrix permeability ratio for Zhang model are definitely different as shown in Fig. 4.

4.2. Impact of local equilibrium assumption

From Figs. 5–7, it is apparent that fracture permeability is also a function of time. Its characteristics indicate that fracture permeability evolution is a dynamic process before whole system reaches its equilibrium state. However, current permeability models ignore this fact. The following analysis shows the dynamic interaction between matrix and fractures and its impacts on evolutions of fracture permeability ratios.

4.2.1. Visualization of the dynamic evolution of fracture permeability

As shown in Fig. 5, the evolution trend of the fracture permeability ratio falls at first then goes up gradually and finally remains steady. Based on this observation, the evolution of fracture permeability ratio is separated into two stages: local swelling and macro swelling. Initially only local swelling controls the fracture permeability then the boundary condition will take effect. Fig. 8 shows

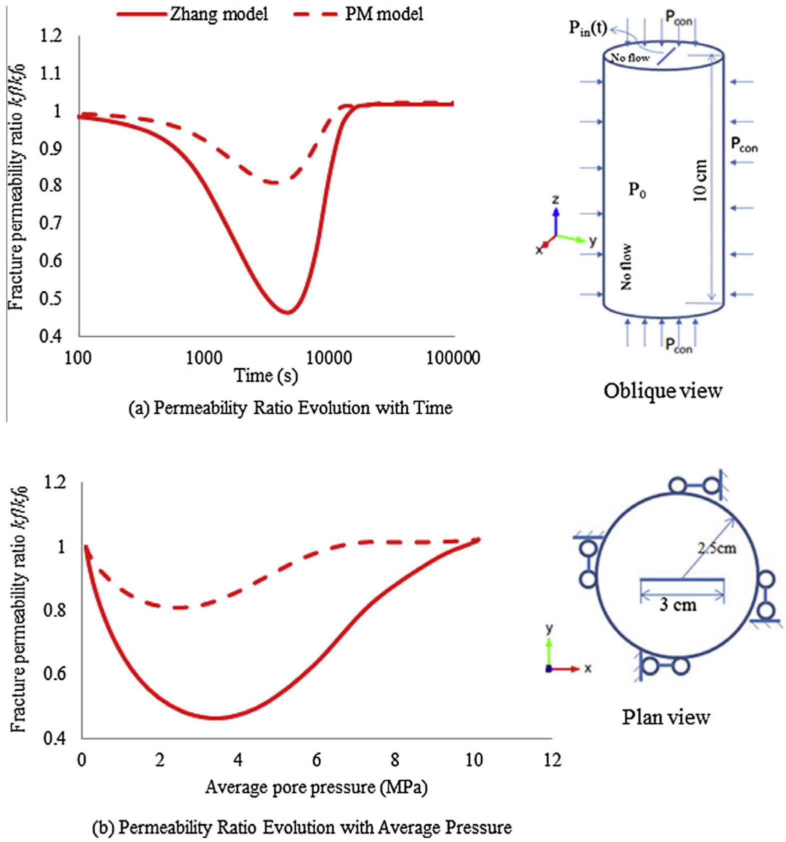

Fig. 5. Comparisons of Zhang model with P&M model under the condition of free swelling.

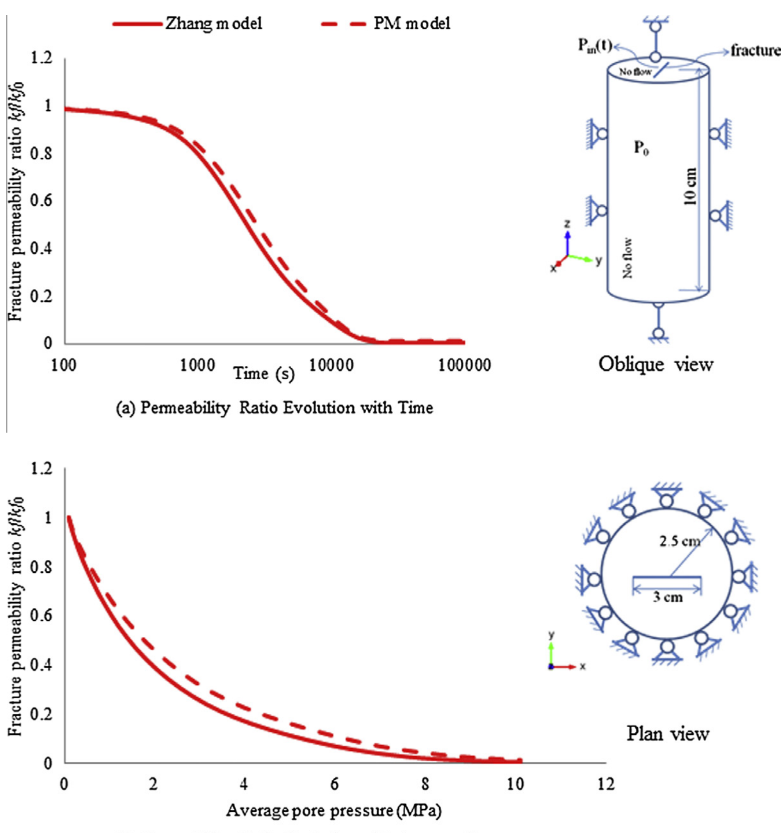

Fig. 6. Comparisons of Zhang model with P&M model under the condition of constant volume.

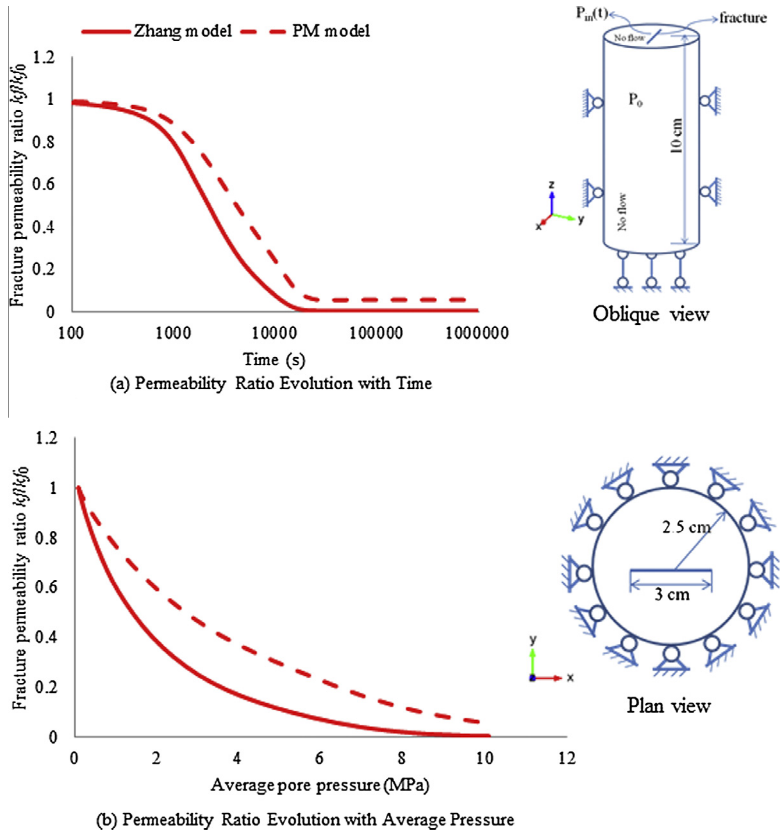

Fig. 7. Comparisons of Zhang model with P&M model under the condition of *z*-direction uniaxial strain.

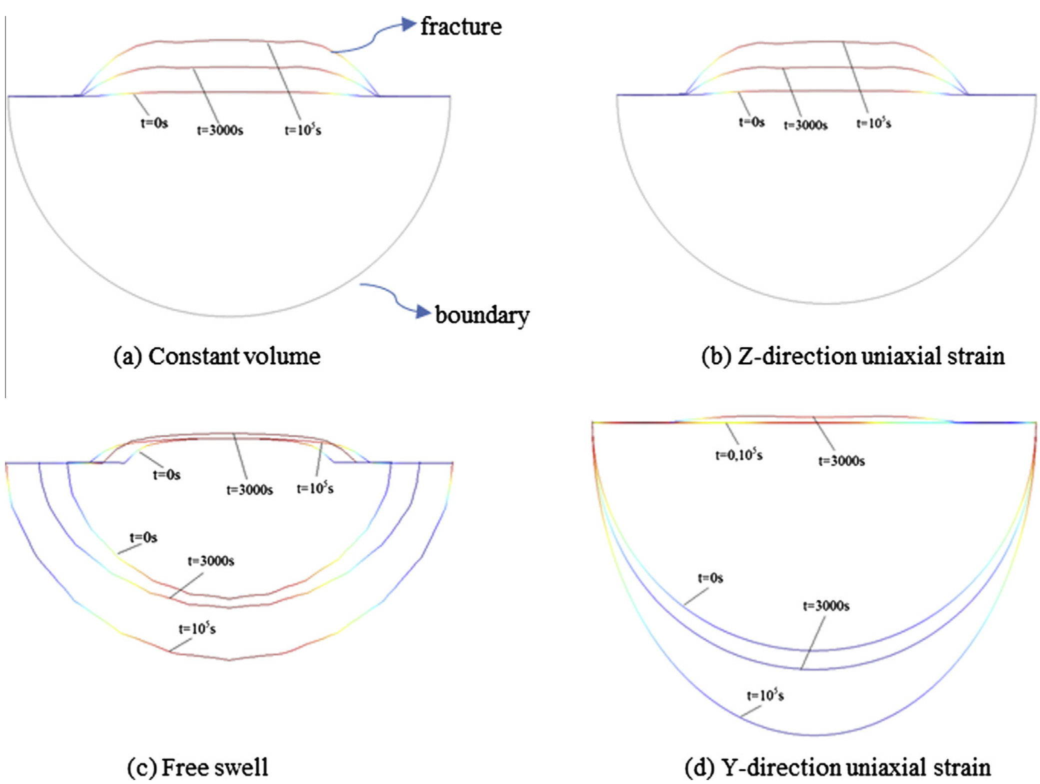

Fig. 8. Evolution of the simulated bottom profile configuration in various boundary conditions.

evolutions of the simulated bottom profile configuration in various boundary conditions. It gives a clear image of the transformation from local swelling to macro swelling. Obviously there is a recovery process and volumetric swelling in the conditions of free swelling and *y*-direction uniaxial strain. From the Fig. 8(c) and (d), it is found that the volumetric swelling is nearly zero before 3000 s and the *y*-direction displacement increment of fracture reaches maximum at 3000 s. Afterwards, the volumetric swelling increases sharply while the *y*-direction displacement of fracture decreases. It is a classic evolution from local swelling to macro swelling. However in the conditions of constant volume and *z*-direction uniaxial strain, the *y*-direction is constrained at the boundary so there is no volumetric strain. The deformation in fracture should only increase without any possibility of recovery.

4.2.2. Deviation caused by the local equilibrium assumption

The boundary of the coal sample under the free swelling condition is commonly used in laboratory. The evolution of the fracture permeability ratio for the free swelling scenario as shown in Fig. 5 is consistent with experimental observations in the Robertson and Christiansen's research [25]. Robertson and Christiansen thought that boundary conditions of samples in laboratory is different to assumed boundary conditions of *industry-standard* permeability models and this difference leads to the mismatch in coal permeability between experimental observations and analytical results. However, we suggest that the dynamic transition of interactions is the real reason. Siriwardane et al. [21] found that increasing exposure time could reduce permeability sharply and the exposure time for such reduction can range from 1.5 days up to a week. Robertson and Christiansen only spent 24 h to equilibrate coal samples. It is highly possible that inside interactions did not cease when permeability was measured. As a result, they even got unacceptable deviations (60% sometimes) after they multiplied P&M model by a variable strain factor.

From our results as shown in Fig. 5, the difference between steady and minimum fracture permeability ratios is huge. The results of the *accurate solution* (Zhang model) indicate that this difference is 54%. It is obvious that if coal samples do not equilibrate inside when measures are taken the deviations between experimental observations and analytical results from permeability models could be huge. Results of Figs. 6 and 7 confirm this conclusion. The maximum deviation between initial and minimum fracture permeability ratios for the constant volume and *z*-direction uniaxial strain scenarios could reach as high as 99%. Therefore, assuming local equilibrium is another main reason that analytical permeability models so far fail to explain experimental observations.

5. Conclusions

In this study, we quantitatively evaluated the performances of coal permeability models under three common assumptions: (1) uniaxial strain; (2) constant overburden stress; and (3) local equilibrium, and those under variable stress conditions. Through these evaluations, we concluded that these three assumptions and their impacts on the evolutions of coal permeability are the main reason why these models have so far failed to explain experimental results from conditions of the controlled stresses, and only partially succeeded in explaining in situ data. In order to better represent the evolution of coal permeability, these three common assumptions must be relaxed through considering the effective stress transfer between matrix and fracture and transforming this stress transfer into the modification of fracture aperture.

Acknowledgements

This work is partially supported by State Key Laboratory of Coal Resources and Safe Mining, China University of Mining and Technology (SKLCRSM11KFA01). This support is gratefully appreciated.

References

[1] Chen Z, Liu J, Elsworth D, Connell LD, Pan Z. Impact of CO_2 injection and differential deformation on CO_2 injectivity under in situ stress conditions. Int J Coal Geol 2010;81:97–108.
[2] Liu J, Chen Z, Elsworth D, Miao X, Mao X. Evaluation of stress-controlled coal swelling processes. Int J coal geol 2010;83:446–55.
[3] Kang SM, Fathi E, Ambrose R, Akkutlu I, Sigal R. Carbon dioxide storage capacity of organic-rich shales. SPE J 2011;16:842–55.
[4] Han F, Busch A, van Wageningen N, Yang J, Liu Z, Krooss BM. Experimental study of gas and water transport processes in the inter-cleat (matrix) system of coal: anthracite from Qinshui Basin, China. Int J Coal Geol 2010;81:128–38.
[5] Wu Y, Liu J, Elsworth D, Miao X, Mao X. Development of anisotropic permeability during coalbed methane production. J Nat Gas Sci Eng 2010;2:197–210.
[6] Palmer I. Permeability changes in coal: analytical modeling. Int J Coal Geol 2009;77:119–26.
[7] Harpalani S, Chen G. Influence of gas production induced volumetric strain on permeability of coal. Geotech Geol Eng 1997;15:303–25.
[8] Gray I. Reservoir engineering in coal seams: Part 1-the physical process of gas storage and movement in coal seams. SPE Reservoir Eng 1987;2:28–34.
[9] Gilman A, Beckie R. Flow of coal-bed methane to a gallery. Trans Porous Media 2000;41:1–16.
[10] Shi J, Durucan S. Drawdown induced changes in permeability of coalbeds: a new interpretation of the reservoir response to primary recovery. Trans Porous Media 2004;56:1–16.
[11] Palmer I, Mansoori J. How permeability depends on stress and pore pressure in coalbeds: a new model. In: SPE Annual Technical Conference and Exhibition; 1996.
[12] Palmer I, Mavor M, Gunter B, Permeability changes in coal seams during production and injection, In: International Coalbed Methane Symposium. University of Alabama, Tuscaloosa. Paper; 2007.
[13] Schwerer F, Pavone A. Effect of pressure-dependent permeability on well-test analyses and long-term production of methane from coal seams. In: SPE Unconventional Gas Recovery Symposium; 1984.
[14] Pekot L, Reeves S. Modeling coal matrix shrinkage and differential swelling with CO_2 injection for enhanced coalbed methane recovery and carbon sequestration applications. Topical Report, Contract No. DE-FC26-00NT40924, US DOE, Washington, DC (November 2002); 2002.
[15] Robertson E, Christiansen R. A permeability model for coal and other fractured, sorptive-elastic media. In: SPE Eastern Regional Meeting; 2006.
[16] Cui X, Bustin RM. Volumetric strain associated with methane desorption and its impact on coalbed gas production from deep coal seams. AAPG Bull 2005;89:1181–202.
[17] Connell L, Detournay C. Coupled flow and geomechanical processes during enhanced coal seam methane recovery through CO_2 sequestration. Int J Coal Geol 2009;77:222–33.
[18] Gu F, Chalaturnyk JJ. Analysis of coalbed methane production by reservoir and geomechanical coupling simulation. J Canad Petrol Technol 2005;44.
[19] Zhang H, Liu J, Elsworth D. How sorption-induced matrix deformation affects gas flow in coal seams: a new FE model. Int J Rock Mech Mining Sci 2008;45:1226–36.
[20] Connell LD, Lu M, Pan Z. An analytical coal permeability model for tri-axial strain and stress conditions. Int J Coal Geol 2010;84:103–14.
[21] Siriwardane H, Haljasmaa I, McLendon R, Irdi G, Soong Y, Bromhal G. Influence of carbon dioxide on coal permeability determined by pressure transient methods. Int J Coal Geol 2009;77:109–18.
[22] Liu J, Wang J, Chen Z, Wang S, Elsworth D, Jiang Y. Impact of transition from local swelling to macro swelling on the evolution of coal permeability. Int J Coal Geol 2011;88:31–40.
[23] Wu Y, Liu J, Elsworth D, Chen Z, Connell L, Pan Z. Dual poroelastic response of a coal seam to CO_2 injection. Int J Greenhouse Gas Cont 2010;4:668–78.
[24] Wu Y, Liu J, Chen Z, Elsworth D, Pone D. A dual poroelastic model for CO_2-enhanced coalbed methane recovery. Int J Coal Geol 2011;86:177–89.
[25] Robertson EP, Christiansen RL. Modeling Permeability in Coal Using Sorption-Induced Strain Data; 2005.
[26] Liu J, Chen Z, Elsworth D, Qu H, Chen D. Interactions of multiple processes during CBM extraction: a critical review. Int J Coal Geol 2011;87:175–89.
[27] Chilingar GV. Relationship between porosity, permeability, and grain-size distribution of sands and sandstones. Develop Sedimentol 1964;1:71–5.
[28] Levine JR. Model study of the influence of matrix shrinkage on absolute permeability of coal bed reservoirs. Geol Soc, Lond, Special Publications 1996;109:197–212.
[29] Clarkson C. Application of a new multicomponent gas adsorption model to coal gas adsorption systems. SPE J 2003;8:236–51.
[30] Laxminarayana C, Crosdale PJ. Role of coal type and rank on methane sorption characteristics of Bowen Basin. Aust coals, Int J Coal Geol 1999;40:309–25.

[31] Levine JR. Influences of coal composition on coal seam reservoir quality: a review. In: Proc. Int. Symp. Coal Bed Methane Resource Develop. Townsville; 1992. p. 1–28.
[32] Pan Z, Connell LD. A theoretical model for gas adsorption-induced coal swelling. Int J Coal Geol 2007;69:243–52.
[33] Clarkson C, Bustin R. The effect of pore structure and gas pressure upon the transport properties of coal: a laboratory and modeling study. 1. Isotherms and pore volume distributions. Fuel 1999;78:1333–44.
[34] Liu H-H, Rutqvist J. A new coal-permeability model: internal swelling stress and fracture–matrix interaction. Tran Porous Media 2010;82:157–71.